

## EXPERIMENTAL APPARATUS TO DETERMINE SPECTRAL EMISSIVITIES OF CERAMIC SAMPLES

**Vicente de Paulo Nicolau, vicente@emc.ufsc.br**

**Daniel Augusto Bernardi Scopel, scopel@labcet.ufsc.br**

**Karen Possoli, k.possoli@gmail.com**

Thermal Science Laboratory  
Mechanical Engineering Department  
Federal University of Santa Catarina  
Florianopolis, Santa Catarina, Brazil

**Abstract.** *An experimental apparatus is assembled in order to measure spectral emissivities of ceramic tiles samples. The measurement system is based on an FTIR spectrometer as the main component, in the wavelength range of 1.7 to 25 micronmeters. Other components include a black-body cavity, a special heater to increase the sample temperature, some optical components and a thermal control system. The black-body cavity is developed based on a typical laboratory kiln, some improvements are executed and the effective emissivity is estimated. Component behaviors are discussed, some measurements are carried out, and normal spectral emissivities results are presented for ceramic and stainless steel samples for distinct temperatures and wavelength ranging from 3 to 25  $\mu\text{m}$ .*

**Keywords:** *thermal radiation, radiant property, spectral emissivity, ceramic tiles*

### 1. INTRODUCTION

Ceramic tiles are generally fired in roller kilns, where the tiles are placed side by side and transported by a sequence of ceramic rollers. These rollers have both the function of support and conveyor, and they are driven by external mechanical devices. A channel over the tile layer is formed by the kiln walls and by the tiles themselves. Another channel is formed under the tiles and rollers and between the kiln walls. During the firing process the tiles attain temperatures of approximately 1200 °C, involving heat transfer processes like convection and radiation. Inside the tiles conduction and other physical-chemical processes occur as the tiles progress through the kiln.

In the thermal simulation of the firing process all these phenomena should be considered, particularly the thermal radiation exchange between the tiles and the kiln environment. Some numerical modeling was performed and applied, and some physical properties are required to accomplish the simulation task. Since thermal radiation plays a significant role, the emissivity is considered as one of the most influencing properties in the heat transfer process. Other surface properties like absorptivity or reflectivity can be calculated using the emissivity values (Incropera and DeWitt, 1996).

As roller kilns have been designed with larger sections, heat transfer to the tiles is needed in order to maintain an isothermal temperature profile across the kiln section. A non-isothermal profile generates a series of dimensional problems, reducing the quality of the fired products. The emissivity plays an important role in the radiation exchange and some coating products of high emissivity are available on the market. Such products should be applied on the kiln walls to enhance the heat transfer (Sheil and Kleeb, 2005), with a consequent reduction in the temperature difference between the central and lateral points of the load.

Several methods available in the literature are used to obtain radiation properties, and they are complementary, since there is no general method valid for every wavelength range and for a wide temperature range. Basically, there are two classes of measurement methods, according to the principle of measurement: radiometric methods and calorimetric methods. Radiometric methods are used to measure the incident, reflected or transmitted radiation, in a particular wavelength range. The ratio of reflected to incident radiation and the ratio of transmitted to incident radiation represent the reflectivity and the transmissivity, respectively. As the ratios are obtained in a particular wavelength range they represent spectral values.

Calorimetric methods consider a situation where there is heat exchange by radiation, for example, between two parallel plates, inside a high vacuum chamber, in order to eliminate heat conduction through the gas between the plates. The heat exchange involved has to be measured and the total hemispheric emissivity is obtained.

Radiometric methods have a wider application, but with some restrictions. Figure 1 shows the field of measurement of reflectivity and emissivity (Sacadura, 1990). For low temperatures, up to 500 K, only the reflectivity can be measured, from 0.3  $\mu\text{m}$  to 15 $\mu\text{m}$ . For higher temperatures and wavelengths above 2  $\mu\text{m}$  one can also measure the directional spectral emissivity. These restrictions apply to low temperatures, since the energy emitted by the surface is quite low, corresponding to the level of energy emitted by the surroundings. This explains why only reflectivity can be measured at low temperatures.

This paper described a useful technique to measure spectral emissivity in the infrared wavelength range. The design of some components and the assembling of the experimental set-up are described and discussed. Finally, some results are obtained for some particular samples.

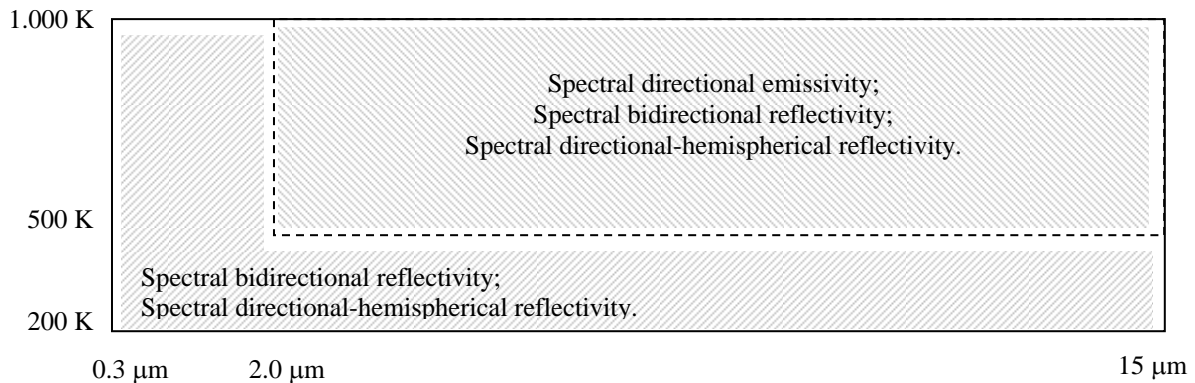


Figure 1. Measurement domain of radiation properties (Sacadura, 1990).

## 2. EXPERIMENTAL APPARATUS

An FTIR spectrometer (Oriel MIR8025<sup>TM</sup> Modular IR Fourier Spectrometer) was used to measure the radiation coming from the sample and compare the radiation intensity with the radiation from a black-body cavity, as depicted in Fig. 2. The beam emitted inside the spectrometer is a collimated beam, with a small divergence angle. The optical set-up includes two spherical mirrors with a curvature radius of 500 mm. The first mirror collects the radiation from the sample or the radiation from the bottom of the cavity. The beam is concentrated onto the diaphragm aperture. The second mirror is placed 250 mm from the diaphragm aperture, which is coincident with the mirror focal distance. The exiting beam reflected by the second mirror toward the spectrometer entrance is then collimated. The diaphragm aperture determines the diameter of the emission area on the sample or on the cavity bottom. As a consequence it determines the divergence angle of the collimated beam introduced at the spectrometer input port and the larger the diaphragm aperture the stronger the signal to be measured. But a limitation is imposed by the cavity geometry and by the spectrometer regarding the spectral resolution.

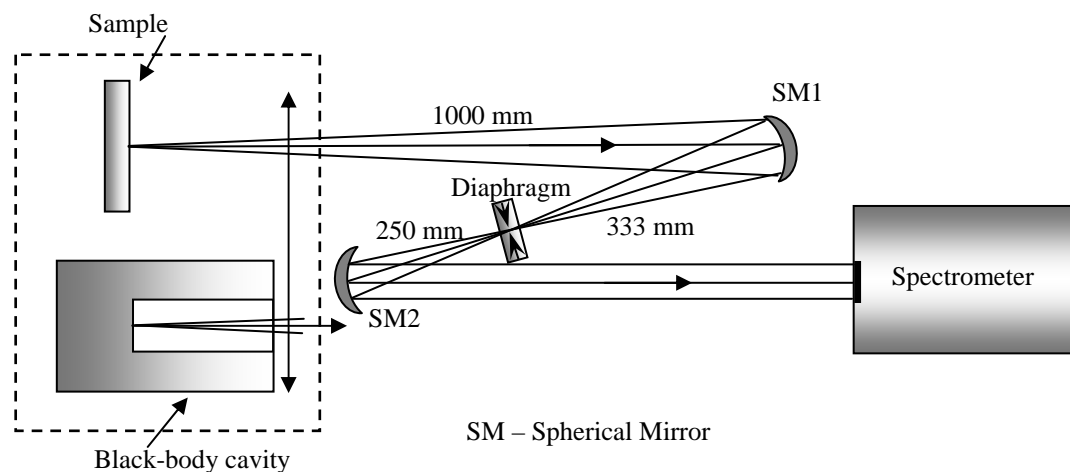


Figure 2. Schematic view of the experimental apparatus.

### 2.1. The spectrometer

The core of an FTIR spectrometer is shown in Fig. 3. It is typically a Michelson Interferometer, with similar components. The input beam strikes a beam-splitter, in such a way that it transmits half of the incident radiation toward the moving plane mirror and reflects the other half toward the fixed-plane mirror. The radiation reflected on both the fixed and moving mirror is combined again on the beam-splitter and constitutes the exiting beam. This recombination can result in a positive or negative interference, depending on the distances travelled by the respective beam, that is,  $2x$

$L_1$  and  $2 \times L_2$  from the beam-splitter to the fixed mirror and to the moving mirror, respectively (Fig. 3). The optical path difference compared to a particular wavelength will define the degree of interference. Since the mirror is moving, distance  $L_2$  is changing and several wavelengths are present, a complex signal is acquired by the detector. The signal is recorded and related to the mirror displacement and a Fast Fourier Transform algorithm is used to find the infrared spectrum (Oriol Instruments, 2001).

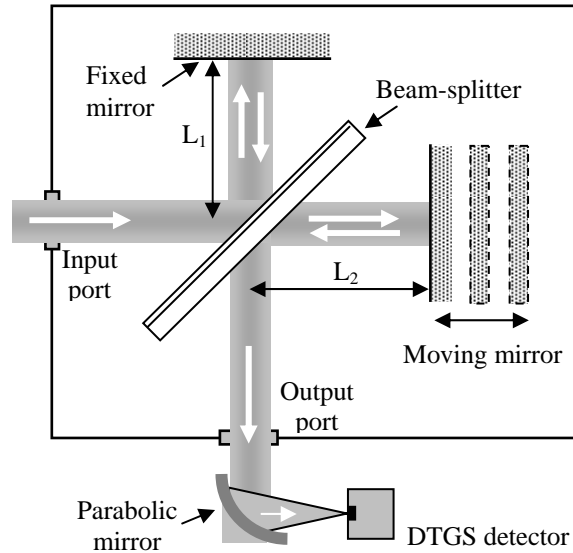


Figure 3 - Schematic view of the core of FTIR spectrometer.

## 2.2. The black-body cavity

The black-body cavity is used as a reference for thermal radiation measurements, in particular for emissivity measurements. Its design considers an internal area/opening area ratio which is as large as possible, a material with a high intrinsic emissivity and a uniform temperature distribution inside the cavity. The exiting beam collected from the aperture, coming from the bottom, parallel to the cavity axis and with a small solid angle around this axis, is used as the reference in the measurement.

A specially designed electric kiln was purchased and adapted to acquire some characteristics of the black-body model. The kiln is cylindrical and a stainless-steel tube is coaxially installed, as shown in Fig. 4. A disc is placed inside the tube, constituting the bottom cavity. The heating element is mounted in an helical form in the space around the tube.

The central circle, named the target or Surface 1, is focalized by the measurement apparatus on the cavity bottom. To evaluate the effective emissivity the cylindrical cavity is divided into  $N$  surfaces, including Surface 1 and the complementary ring on the bottom, several discretized rings on the lateral wall and the aperture. All the surfaces contribute to establishing an internal radiating field and an effective emissivity can be defined, with a resulting value between the wall emissivity value and unity, depending on the cavity performance.

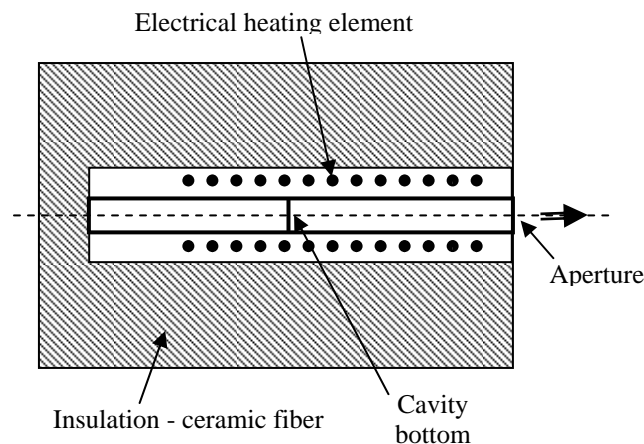


Figure 4. Components of the black-body cavity.

The radiant flux incident to the target (Surface 1) is calculated using Eq. (1). The model adopted is the net-radiation model, which considers the surfaces as diffuse and gray surfaces.

$$q_{inc,1} = \sum_{i=1}^N \sigma A_1 G_{1,i} T_i^4 \quad (1)$$

where  $\sigma$  is the Stefan-Boltzmann constant,  $A_1$  is the area of Surface 1 and  $T_i$  is the temperature of each surface component of the cavity model.  $G_{1,i}$  is the Gebhart factor, which represents the fraction of the emission from all the discretized cavity surfaces that reaches Surface 1 directly or by multiple reflections and is absorbed (Siegel and Howell, 1992).

As Surface 1 is a non-black surface, some radiation is reflected. The absorbed radiation can be estimated, multiplying Eq. (1) by the respective emissivity. Reflected radiation is obtained through the complement, as presented in Eq. (2).

$$q_{refl,1} = \sum_{i=1}^N \sigma A_1 (1 - \varepsilon_1) G_{1,i} T_i^4 \quad (2)$$

The emitted radiation flux is calculated using Eq. (3).

$$q_{em,1} = \sigma A_1 \varepsilon_1 T_1^4 \quad (3)$$

The total radiation flux leaving Surface 1 is estimated through Eq. (4).

$$q_{refl+em,1} = \sum_{i=1}^N \sigma A_1 (1 - \varepsilon_1) G_{1,i} T_i^4 + \sigma A_1 \varepsilon_1 T_1^4 \quad (4)$$

The energy leaving Surface 1 can be expressed using an effective emissivity as presented in Eq. (5).

$$q_{eff,1} = \sigma A_1 \varepsilon_{eff,1} T_1^4 \quad (5)$$

Comparing Eqs. (4) and (5), the effective emissivity can also be obtained in Eq. (6).

$$\varepsilon_{eff,1} = \left( \sum_{i=1}^{N+2} (1 - \varepsilon_1) G_{1,i} T_i^4 + \varepsilon_1 T_1^4 \right) / T_1^4 \quad (6)$$

This effective emissivity is the ratio between the target radiosity (emitted and reflected radiant flux) and the radiation emitted from the black surface of area  $A_1$  and temperature  $T_1$ .

The cavity has a diameter of 34.0 mm and is 290 mm long. The stainless steel tube has a wall 2.0 mm thick and is oxidized. A special ceramic coating (HiE-Coat 840M) is used to improve the surface emissivity, estimated as 0.9, and it sustains temperatures as high as 1100 °C. The temperature profile along the cavity wall was measured and is presented in Fig. 5. As a uniform temperature is expected, some improvements should be carried out in this case to approximate the black-body model. The electrical heating element can be moved toward the cavity entrance and a tube with a thicker wall can be used in order to obtain a more isothermal surface.

Using the temperature distribution for the cavity wall, as shown in Fig. 5, and Eq. (6), an effective emissivity equal to 0.99 can be achieved. This value is specifically for a radiation beam coming from the bottom of the cavity.

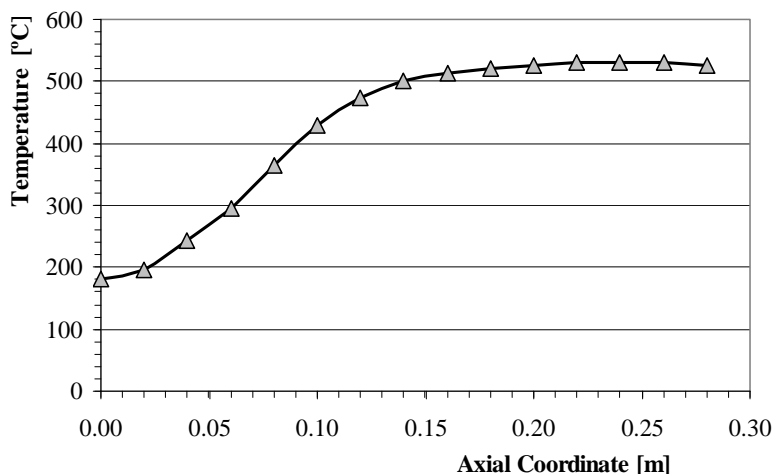


Figure 5. Temperature distribution of the cavity wall.

### 2.3. Energy availability and emissivity uncertainty

The radiant energy available to perform a specific spectral emissivity measurement is limited by the temperature of the sample, and by the spectral distribution of the radiant energy itself. Figure 6 shows the spectral emittance for a theoretical black-body cavity, given by the Planck distribution function (Siegel and Howell, 1992). The curves are normalized in order to compare the temperature influence on the spectral distribution. This is necessary because the maximum spectral emittance for  $T=800\text{ K}$  is 32 times greater than the respective value for  $T=400\text{ K}$ .

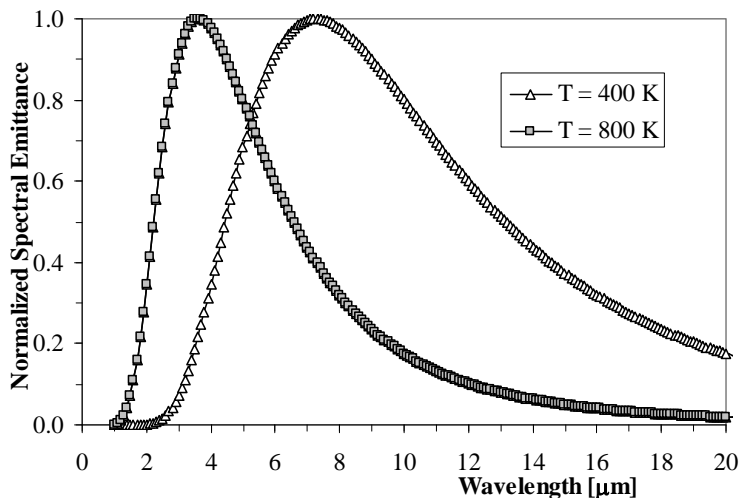


Figure 6. Normalized spectral emittance for distinct temperatures.

Observing the curves in Fig. 6, it seems that there is not enough energy to measure at shorter wavelengths, mainly for  $T = 400\text{ K}$ . For this temperature it is necessary to go beyond  $3.0\ \mu\text{m}$ , as the fraction of accumulated energy before this wavelength represents only 0.27 % of the total emitted energy. For higher temperatures the curve of spectral emittance shifts toward shorter wavelengths; e.g. for  $T=800\text{ K}$ , 2.33 % of the total emitted energy lies before  $3.0\ \mu\text{m}$ .

Although Fig. 6 presents normalized curves, it is known that at higher temperatures more energy is emitted, as previewed by Stefan-Boltzmann's fourth power law. This proportion is not directly verified in a spectral base, because there is a displacement toward shorter wavelengths when the temperature is increased. A sample at higher temperature represents more energy available and consequently less noise in the measurement process. However, a drawback to increasing the temperature is the control and obtainment of an isothermal sample.

As the emissivity is the ratio of sample to black-body spectral emittances, both of them need to be controlled in order to achieve a stable temperature. A small temperature difference results in uncertainty in the emissivity. This

uncertainty is estimated based on Planck's Law and some results are available in Fig. 7. A temperature uncertainty of 0.5 % is considered in the analysis. It can be seen that spectral emittance is more sensitive to temperature variations for short wavelengths. The first point is that the peak of maximum emission changes with the temperature in value and position. The second point to be considered is the left side of the curve with a high slope and a strong dependence on the temperature resulting in a similar dependence on the uncertainty. For the far infrared region all the spectral emittance curves are progressively reduced as the wavelength increases and the uncertainty undergoes a relative reduction.

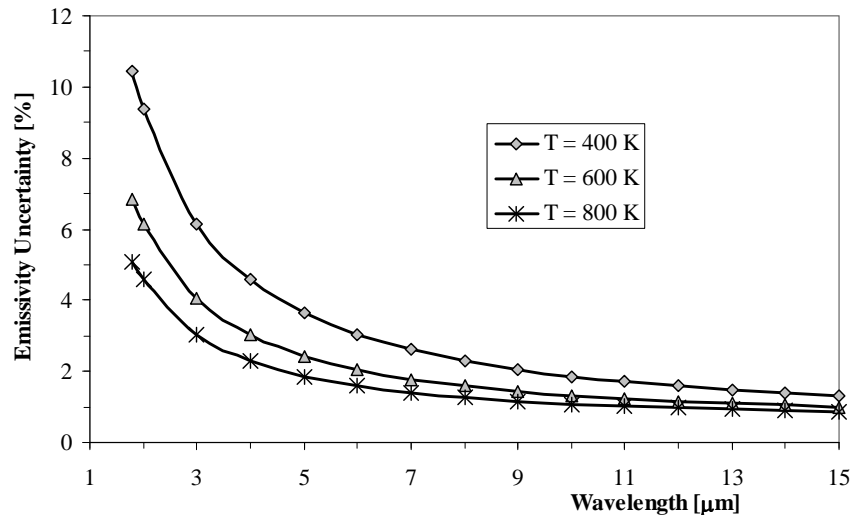


Figure 7. Spectral emissivity uncertainty based on a temperature uncertainty of 0.5 %.

### 3. RESULTS

Some preliminary results relating to the ceramic sample and a stainless steel sample are given in Figs. 8 and 9. The ceramic sample is a 10 cm by 10 cm enamel wall tile, with 6 mm thickness and a blue colour. The stainless steel sample is a semi-oxidized disc of 32 mm diameter and 3 mm thickness. Several spectral resolutions were tested and the results for two of them ( $64 \text{ cm}^{-1}$  and  $16 \text{ cm}^{-1}$ ) are shown in Figs. 8 and 9, respectively. The results indicate that these resolutions are adequate to perform the measurements. The finest resolution available is  $0.5 \text{ cm}^{-1}$ , but it takes more time to scan the spectral range. In addition, the details of the spectral absorption bands of the  $\text{CO}_2$  and water vapour, present in the room environment and consequently in the beam, can blur the acquired spectra for the black-body and for the sample measurements. During the acquisition time several scans can be added in order to reduce the noise/signal ratio.

The ceramic material showed a high spectral emissivity of around  $6 \mu\text{m}$ . As presented by De Bellis (1991), such an increase in the emissivity is very characteristic of ceramic materials, probably due to the absorption bands of the silica (in our case silica is an important component of the enamel layer). After this peak a strong reduction is observed for longer wavelengths, up to  $9 \mu\text{m}$ , remaining almost constant thereafter. Another reduction is observed after  $18 \mu\text{m}$ , but the available energy is very low in this complementary spectral range, as plotted in Fig. 6. Some variations in the spectral emissivity values are also observed, when different temperatures are used in the measurement. Temperatures lower than  $400 \text{ }^\circ\text{C}$  were also used, but a high level of noise was observed and non conclusive data were obtained.

The stainless steel sample was also measured resulting in lower emissivities, as shown in Figs. 8 and 9. Very low emissivities were observed in the  $11$  to  $17 \mu\text{m}$  wavelength range, although more measurements need to be taken to confirm this tendency. An improvement in the emissivity values should occur as the surface becomes more oxidized and this also needs to be verified.

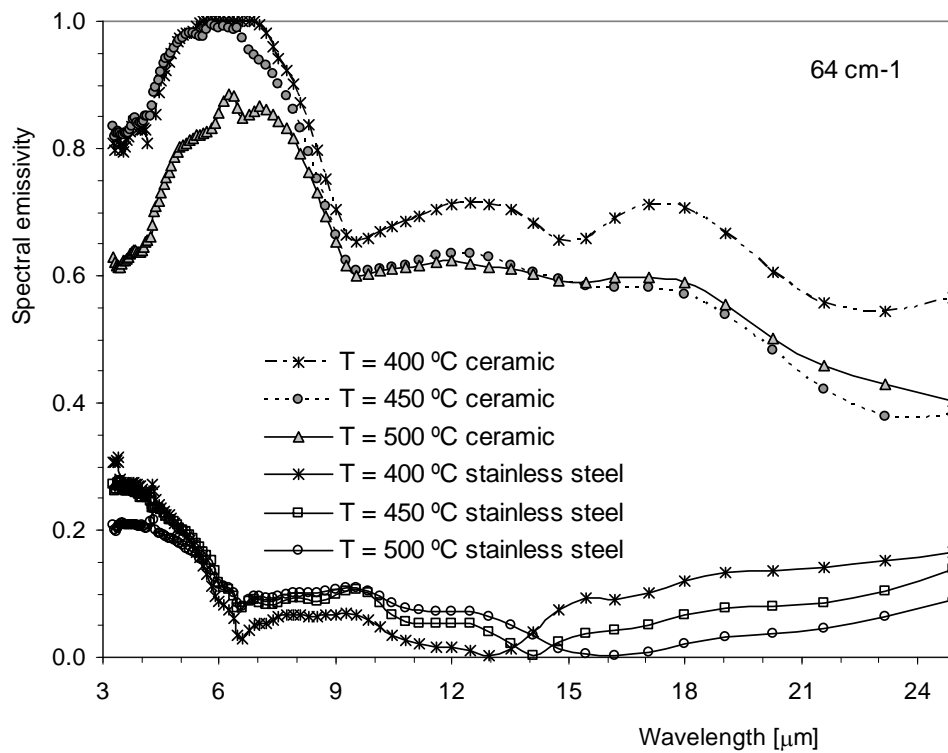


Figure 8. Normal spectral emissivity for ceramic and stainless steel samples, resolution = 64 cm<sup>-1</sup>.

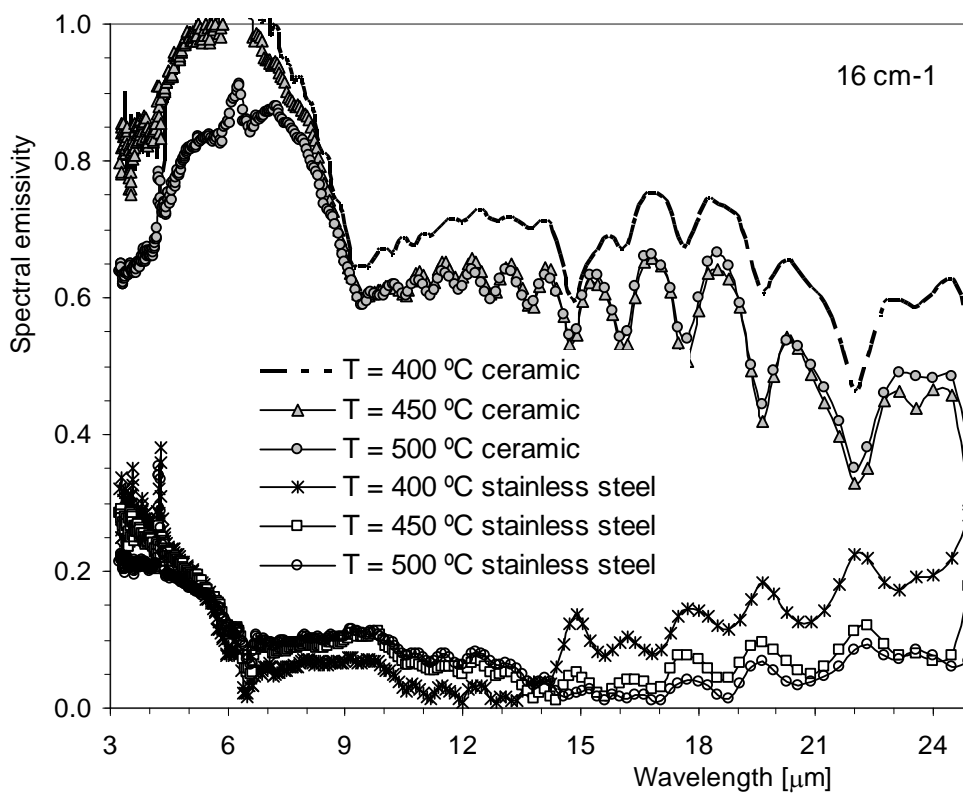


Figure 9. Normal spectral emissivity for ceramic and stainless steel samples, resolution = 16 cm<sup>-1</sup>.

#### **4. CONCLUSIONS**

An experimental apparatus has been described and used to measure the normal spectral emissivity of ceramic samples in the infrared wavelength range. A modular and versatile FTIR spectrometer was acquired with the source and detector in separated modules, in order to give more flexibility when a distinct set-up is required. One of the most restrictive characteristics, the alignment of the components, could be fitted satisfactorily. Other set-up components, like the black-body, sample heating and control system, are under development, and the measurements show some encouraging results. However, some improvements need to be incorporated in order to achieve a higher temperature level with a finer control.

#### **5. ACKNOWLEDGEMENTS**

The experimental set-up was funded by Petrobrás S.A. The author D.A.B. Scopel has a grant from the “Programa de Recursos Humanos da ANP para o Setor de Petróleo e Gás Natural- PRH09-ANP/MME/MCT”.

#### **6. REFERENCES**

- Acimac, Associazione Costruttori Italiani Macchine Attrezzature per Ceramica, 2005, “Drying and Firing of Ceramic Tiles”, Modena, Italy, 448p.
- De Bellis, C.L., 1991, “Effect of Refractory Emittance in Industrial Furnaces”, *Fundamental of Radiation Heat Transfer*, ASME HTD, vol 160, pp. 105-115.
- Incropera, F.P. and DeWitt, D.P., 1996, “Fundamentals of Heat and Mass Transfer”, John Wiley, New York, 884 p.
- Oriel Instruments, 2001, “The Book of Photon Tools”, Stratford, CT, USA, pp.5.1-5.38.
- Sacadura, J.F., 1990, “Measurement Techniques for Thermal Radiatives Properties”, *Proceedings of the 9th International Heat Transfer Conference*, vol 1 KN-12, Jerusalem, pp 207-222.
- Sheil, P.C. and Kleeb, T.R., 2005, “High Emissivity Coatings for Improved Performance of Electric Arc Furnaces”, *Proceedings of the AISTech 2005 - Iron and Steel Technology Conference*, Charlotte, North Carolina, 6 p.
- Siegel, R. and Howell, J.R., 1992, “Thermal Radiation Heat Transfer”, Hemisphere Publishing, 3rd. Ed., New York, 1072p.

#### **7. RESPONSIBILITY NOTICE**

The authors are the only people responsible for the printed material included in this paper.